Electric Power Systems Research 226 (2024) 109923

Contents lists available at ScienceDirect

Electric Power Systems Research

journal homepage: www.elsevier.com/locate/epsr

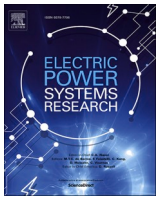

Tri-level hierarchical coordinated control of large-scale EVs charging based on multi-layer optimization framework

Tawfiq Aljohani [a,*], Mohamed A. Mohamed [b], Osama Mohammed [c]

[a] Department of Electrical Engineering, College of Engineering at Yanbu, Taibah University, Yanbu Al-Bahr 41911, Saudi Arabia
[b] Electrical Engineering Department, Faculty of Engineering, Minia University, Minia 61519, Egypt
[c] Energy Systems Research Laboratories, Florida International University, Miami, FL 33174, USA

ARTICLE INFO

Keywords:
Electric vehicles
Mixed-integer quadratic programming (MIQP)
Hierarchical energy management
Stackelberg model
Energy markets
EVs dynamic charging

ABSTRACT

The stochastic nature of electric vehicles (EVs) has made predicting and ultimately controlling their integration on a large scale a very challenging task. This work proposes a two-layer optimization framework based on the Stackelberg leader and follower to manage a tri-level energy management strategy to coordinate EVs charging. The first layer incorporates an aggregator that collects the energy requirements of all EVs in a decentralized manner, and sends them to an attached microgrid, which constitutes the second layer of the proposed scheme, for further processing. Then, the microgrid runs a lower-level energy optimization problem in a centralized manner based on the inputs from its aggregators downstream and a system operator upstream, which operates in the third level. Simultaneously, the coordination between the system operator and its attached microgrids is formulated as an upper-level energy optimization problem. The work incorporates the dynamics of the energy system by modeling practical economic, technical, and operational variables. The formulated problem is solved via mixed-integer quadratic programming (MIQP). The results show that the proposed strategy has successfully influenced the charging requirements of EVs due to the dynamic energy price signals issued following the system's timely operation. In addition, the results demonstrated an optimal energy exchange to support optimal operation and reduce overall costs.

1. Introduction

Major restructuring of industries that significantly contribute to global GHG emissions is continually in progress. Plug-in Electric Vehicles (EVs) are seen as key tools in the significant restructuring of major contributors of emissions, the electric power industry, and the transportation sector [1]. Large-scale penetration of EVs is considered as a major challenge, as their uncoordinated charging will lead to various technical and operational power system problems such as increased peak loads and losses, excessive voltage drops, and overloaded feeders [2]. Research has been intensified in the last decade on energy management and control to properly manage large-scale integration of EVs. Recent literature has studied the impact of uncontrolled charging of a large population of EVs [3]. The authors in [1] provide a study on integrating a one-million EVs into the VACAR sub-region of the Southeast Electric Reliability Council (SERC). The study considered various charging and discharging scenarios with different EV sizes, energy requirements, and time of connectivity and concluded that a typical residential power distribution feeder will not withstand charging EVs for long hours without causing severe overloadings and possible outages. In [2], the authors present one of the earliest research studies on the grid's impact of uncoordinated EVs integration, where they investigated the impact of integrating 7.5 million EVs on the technical, economic and operational aspects of the power grid. They concluded that unless large-scale EVs loads are managed to be delayed from peak hours to off-peak hours, a substantial increase in energy prices is inevitable in several areas within the US interconnected network. In [3], the authors tested the impact of the uncoordinated large-scale adoption of EVs on the hourly operation of the power distribution grid. Specifically, the authors simulated different testing scenarios to dynamically model the hourly impact of EVs integration considering different EVs types and energy needs. According to their results, uncoordinated large-scale integration of EVs will violate the system's voltage limits and lead to overloading conditions and increased energy prices for all consumers connected to the distribution feeder. Additionally, the study introduced in [4] concluded that simple charging strategies yield peak demands in

* Corresponding author.
E-mail address: torwi@taibahu.edu.sa (T. Aljohani).

https://doi.org/10.1016/j.epsr.2023.109923
Received 10 March 2023; Received in revised form 23 September 2023; Accepted 8 October 2023
Available online 20 October 2023

several time slots of the day, which require significant investment to upgrade the system's overall generation and transmission capacities. Therefore, proper energy management is needed to deal with the uncertainty of the large-scale integration of EVs.

Several methodologies have been proposed recently to deal with the challenging task of accounting EVs load into the already-congested power grid. The authors in [5] proposed a two-step framework to coordinate the EVs charging following price-based coordination based on linear programming. In [6], the authors proposed a methodology that accounts for the design of grid-interfaced EV-charging system incorporating stochastic renewable energy sources and storage units into the electrical infrastructure. The authors utilized a linear programming-based framework to reduce the system's lifecycle cost. Regardless, efforts are still needed to cover the research gap that investigates the impact of large-scale integration of EVs on both economic and technical aspects.

Unintended periods of simultaneous charging at multiple charging stations without proper coordination of multiple aggregators can lead to a severe negative impact on the grid operation. However, most of the proposed methodologies ignored important factors that resemble realistic operations and dynamics of an interconnected energy system. The authors in [7] proposed a hierarchical strategy that prioritizes EVs charging based on available demand using the entropy weight method. However, the authors neglected the fact that demands must be met if drivers plugged their EVs into the grid. The authors in [8] proposed an aggregator-based hierarchical control mechanism for second-order frequency control using optimal EVs scheduling. In the proposed solution, the EV planning considered meeting energy needs with frequent bidirectional energy transfers to the grid. Yet, the solution neglected the dynamics of the interconnected system and the variations of the generation systems, supply and demand levels, and energy exchange within the interconnected system. The authors in [9] proposed mixed-integer linear programming to solve community energy management system to reduce operational costs with adjustable generating units on sites and energy trading. However, important factors such as the scarcity cost of generation units, operational costs associated with energy exchange between microgrids, carbon emissions and renewable portfolio standard (RPS) were not considered. Other studies considered market dynamics in their proposed hierarchical energy management structures such as game theory [10], and model predictive control [11] but yet neglected important variables such as energy exchange, thermal runaway (TR) loadings, carbon emissions, RPS and costs associated with energy exchange to be reflected on the actual EV charging price. Additionally, hierarchical coordination was developed to solve general energy management problems following either price-based or schedule-based coordination, whereas decentralized charging mechanisms are mainly built on the price-based concept. Limited research has considered any form of dynamic charging, which should be the main cornerstone in such problems. The main contributions of the proposed work in this manuscript are as follows:

1 A two-layer (upper and lower) quadratic optimization formulation considering the Stackelberg model is proposed to incorporate timely decisions for three layers of the control scheme. This scheme reflects continuously updated real-time energy price signals that influence consumer behavior, while distinguishing between EVs and non-EVs loads for fair pricing allocations.
2 To solve the proposed methodology, this work develops mixed-integer quadratic programming (MIQP) that consider important variable for realistic modeling of energy market operations such as RPS standards and carbon credits.
3 To the best of our knowledge, the previously proposed literature considered either assumed or used Time-of-Use (ToU) rates as energy pricing schemes in their modeling. Such assumptions may constitute a serious flaw as the impact of a sudden large EVs population may influence the price signal and drive it higher than expected, which is not properly captured if ToU or artificial rates are utilized. This work incorporates dynamic energy pricing that follows changes in real-time demands and level of supply.
4 In addition to point 3, this work integrates practical variables that are essential to model the dynamic and realistic operation of the energy grid. To the best of our knowledge, most of these variables are neglected in previous literature. Such variables include the willingness-to-pay factor (WTP) of consumers, wheeling charge that resembles the real cost of exchanging energy in an interconnected system, social welfare of the EV's owners, RPS, carbon credits and emission rates, limits and capacity of energy of the transmission line between microgrids, elasticity price as a result of energy levels changes, and scarcity rent of the generation units.

This paper is arranged as follows: Section 2 illustrates the proposed tri-level hierarchy; Section 3 presents the problem formulation for the two layers of energy optimization; Section 4 presents case studies and results; Section 5 concludes this work with final remarks.

2. The proposed tri-level hierarchical energy management methodology

2.1. The inverse-demand curve

Consumers in energy markets are expected to react naturally to price fluctuations that influence their decision to use services when they need them. This behavior is well characterized by the inverse demand curve (IDC) that determines energy prices at all generation (supply) and demand (load) levels of the electrical system. Additionally, the IDC represents the consumer's willingness to pay extra to get power within a specific time period. This is known as the WTP coefficient and indicates the marginal utility consumers receive if they use additional energy services. Following a well-known rule of microeconomics, these marginal utilities are estimated using the magnitude of utility required for the total amount of products and energy services available during a given period of our study. Logically, consumers can extend their marginal utility through energy consumption until the marginal utility equals the energy market price. Then at specific points, it would be uneconomical to continue utilizing the energy. This stems from a basic microeconomic fact that when supply is limited, the cost of a product gradually increases. Such total costs, also called marginal costs, reflect other factors related to market conditions. Factors such as power generation levels, fuel supply, operational constraint violations, RPS, and CO_2 limits are included in this work. These variables affect the marginal cost, especially in the short term, that characterizes the power grid's daily and weekly operation.

On one hand, EVs owners are considered regular consumers of the electrical energy needed to charge their vehicles on a daily basis. However, the different energy utilization patterns are attributed to individual EV owners. Such patterns are characterized by several factors that are determined only by the owner of the EV, such as driving patterns, personal habits (e.g., travel, and outdoor activities), work, vehicle type, etc. Therefore, each EV would require a certain level of energy consumption in a decentralized manner. On the other hand, the power production companies are almost heterogeneous regarding the energy's cost structure. Specifically, each generation unit has its own technical and operational status that defines its energy output's price signal. Usually, these generation units run under certain circumstances that increase their price signal. Such circumstances include generation capabilities per unit, environmental policies that govern the generation process to meet specific emissions standards, and regulations that require the utility to incorporate RPS goals, among other factors effectively contributing to determining the level of supply of a power utility. Therefore, accurate broadcasting of the energy prices must reflect the timely condition of both the supplier (the power utility or system operator) and consumer (EVs owners). There is a scarcity of literature to

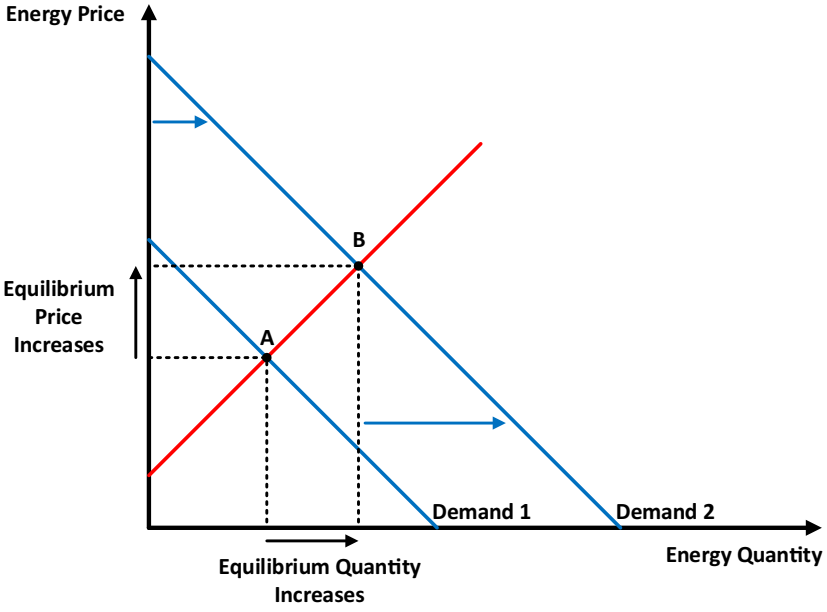

Fig. 1. Illustration of the inverse-demand concept in energy pricing.

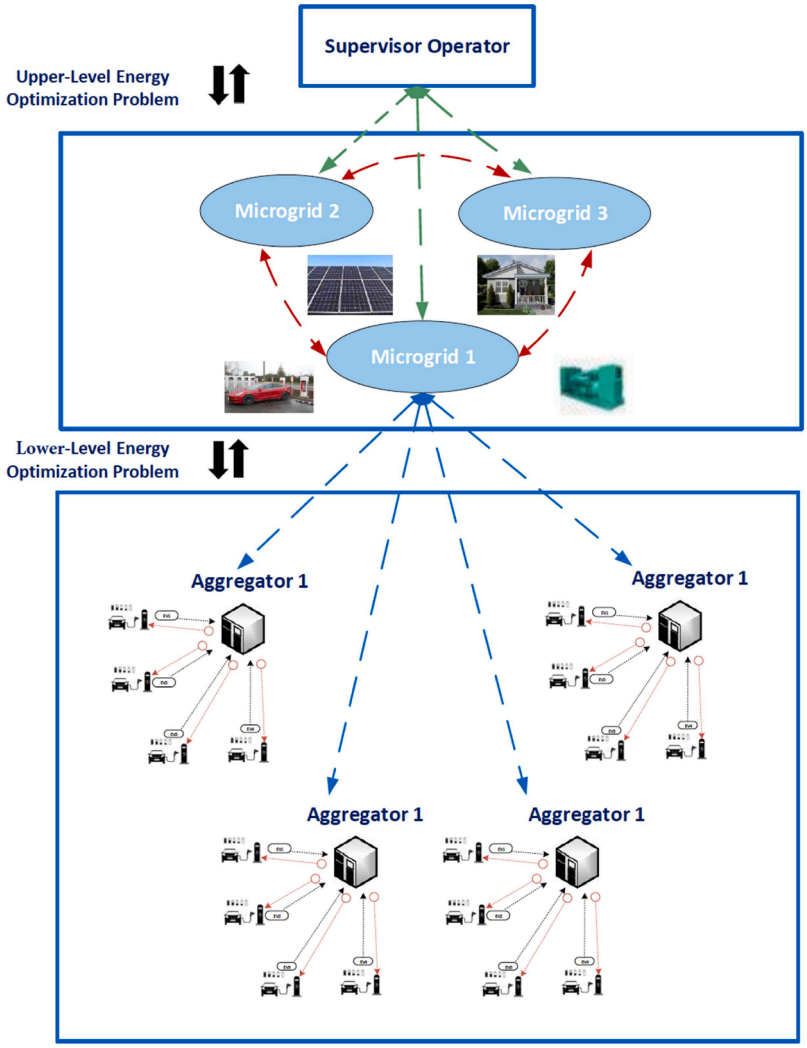

Fig. 2. Schematic illustration of the proposed tri-level scheme.

model such a meaningful relationship that is well-captured by the IDC. Furthermore, this work sees the IDC as an effective modeling strategy that better describes the minute-to-minute modernization of the electric network operation, resulting in accurate and reliable energy price signals considering the large-scale integration of EVs. Therefore, the concept of the tri-level hierarchical control framework proposed in this work is mainly built on establishing price signals following the availability of supply levels determined by the IDC curve, as illustrated in Fig. 1.

2.2. Hybrid centralized-decentralized EVs charging coordination

This work utilizes coordination schemes of both decentralized and centralized management paradigms, based on predetermined duties allocated to different players in the decision process. Such players include aggregators at the station level, microgrid agents, and a system operator overseeing the energy grid's generation and operation capabilities. Specifically, information about the EVs is collected in a decentralized manner from EVs owners (such as the arrival and requested departure times, desired level of energy, … etc.). The collected information is processed through an aggregator. This aggregator collects all connected and request-to-connect EVs' energy and power requirements and sends them to its attached microgrids for further processing. Then, the microgrid runs the lower-level energy optimization problem in a centralized framework based on inputs from both downstream aggregators and an upstream system operator. The coordination between the system operator and its attached microgrids is solved as the upper-level energy optimization problem, formulated following the Stackelberg leader and follower concept. Moreover, the tri-level problem is then modeled based on MIQP, which considers the carbon emissions cap-and-trade policies and the RPS requirement from local authorities and other economic variables that are essential to the accurate determination of energy price signals. Fig. 2 presents a schematic description of the proposed tri-level energy management system.

2.3. The stackelberg model for EVs charging coordination

The concept of the Stackelberg model is based on multi-period dynamic games, where two players sequentially decide their strategic moves rather than simultaneously. Typically, the leader starts with the first move based on knowledge and anticipation of its follower's reaction. Once the leader's move is intact, the follower then makes a strategic decision in the sequential period of the leader's first move. Such a process could be modeled as a bi-level optimization problem considering the sequential trends in issuing decisions. In this work, such strategic moves represent the grid's operation considering large-scale EVs charging. Specifically, the system operator will act in this scenario as a leader that solves its revenue-maximization optimization model based on the knowledge of the operation of its attached microgrids. As followers, microgrids make strategic decisions based on their lower-level optimization problem information with the EVs station aggregators.

3. Mathematical formulation of the proposed tri-level hierarchical energy management strategy

3.1. Mathematical formulation of the lower-level (hybrid centralized-decentralized EVs charging coordination)

Suppose that there is a large group of EVs that are looking to charge over a multi-period timeslot $\Im = \{0, \ldots, T-1\}$. The state of charge (SoC) of an EV$_{\nu}$ that would like to connect to an aggregator j under microgrid i is modeled as follows:

$$SoC_{ijn}(t+1) = SoC_{ijn}(t) + \frac{\eta_n^{ev}}{B_{ijn}} D_{ijn}^{EV} \tag{1}$$

Where η_n^{ev} symbolize the charging efficiency of EV$_{\nu}$ such that $\eta_{ijn}^{EV} \in [0,1]$, B_{ijn} is the EV battery's energy capacity, and D_{ijn}^{EV} represents the charging power demanded by the νth EV at an aggregator j under a microgrid i, and is indicated by the kW needs of the vehicle such that:

$$D_{ijn}^{EV}(t) = D_{ijn}^{EV}(t);\ t \in \Im \tag{2}$$

$$\sum_{t\in\Im} D_{ijn}^{EV}(t) = \sum_{n\in N_{ijn}^{t}} \frac{B_{ijn}}{\eta_{ijn}^{EV}} \cdot \left[SoC_{ijn}^{dept\_mx} - SoC_{ijn}^{a} \right] \tag{3}$$

Where SoC_{ijn}^{a} and $SoC_{ijn}^{dept\_mx}$ are the arrival and maximum possible SoC of EV$_{\nu}$. B_{ijn} is highly dependent on the driving distance, driving speed, EVs' type, and road and traffic conditions. Moreover, the charging power is admissible to a charging station with an aggregator j if:

$$D_{ijn,t}^{EV} = \begin{cases} \in \left[-\zeta_{ijn}^{-}, \zeta_{ijn}^{+} \right], & t \in I \\ = 0, & otherwise \end{cases} \tag{4}$$

Where $\zeta_{ijn}^{-}, \zeta_{ijn}^{+}$ are factors that resemble the uniform rate of charging and discharging power over time. Additionally, the charging needs of an EV must be fully satisfied as follows:

$$\eta_{ijn}^{EV} \cdot \sum_{k=0}^{T_{ijn}-1} D_{ijn}^{EV}(t+k).\Delta + SoC_{ijn}(t).B_{ijn} = SoC_{ijn}^{dept}.B_{ijn} \tag{5}$$

Additionally, the capacity of the power distribution transformer connected to aggregator j must be within the safe limit so that the accumulated charging demands of EVs do not cause overloading:

$$\sum_{n\in N_{ijn}^{t}} \sum_{t\in\Im} D_{ijn}^{EV}(t+k) \le M_{ij}.\sigma_{ij}(t+k) \tag{6}$$

$$\left[SoC_{ijn}^{dept} - \vartheta_n \right].B_{ijn} \le \eta_n^{ev} \cdot \sum_{k=0}^{T_{ijn}(t)-1} D_{ijn}^{EV}(t+k).\Delta + SoC_{ijn}^{a}.B_{ijn} \le SoC_{ijn}^{dept}.B_{ijn} \tag{7}$$

Let us consider a microgrid i that is connected to a system of microgrids and all operating under a unified system operator [12]. Each microgrid i has G generation units such that ($g \in G_i$), with each g having generation capacity ($\mathscr{X}_i^g$) as well as associated marginal costs (C_i^g). The centralized objective function to be solved at the microgrid i level during timeslot t is formulated as follows:

$$J = J_1 + J_2 + J_3 + J_4 + J_5 \tag{8}$$

The first objective function, J_1, accounts for the integration of the area beneath the IDC for the base demand (non-EVs load) on microgrid i, denoted D_i^{Base}, given the instantaneous marginal cost $C_i^{'}$, as follows:

$$J_1 = \left[C_i^{'}(t+k).D_i^{Base}(t+k) - \frac{C_i^{'}(t+k)}{2\Gamma_i(t+k)} \left[D_i^{Base}(t+k)^2 - \sum_{J\in J_i} \sum_{g\in G_i} x_i(t+k)^2 \right] .\Delta \right] \tag{9}$$

Where Γ_i is the cumulative capacity of microgrid i in MW, represented as the x-axis of the inverse-demand curve. Δ is the number of hours considered to normalize the capacity of the generation units. The importance of this function is to model the energy price with respect to the change of demand of non-EVs loads on microgrids. The second objective function, J_2, accounts for the integration of EVs load demand at the timeslot of interest beneath the IDC, given microgrid i operational costs obtained as a result of aggregator j for EV scheduling, as follows:

$$J_2 = \left[b_{ij}^{'}(t+k).D_{ijn}^{EV}(t+k) - \frac{b_{ij}^{'}(t+k)}{2\Gamma_i(t+k)} \left[\sum_{n\in N_{ijn}^{t}} D_{ijn}^{EV}(t+k)^2 \right] .\Delta \right] \tag{10}$$

The third objective function J_3, accounts for the adds-on prices resulting from capacity scarcity exchange between interconnected

microgrids *i and m*. Someone can look at this price as the compensation for the capacity remuneration for being available to another market participant:

$$J_3 = [\mathrm{Y}^{g}_{mi}(t)[x^{g}_{mi}(t) - \mathscr{X}^{g}_{mi}(t)]\Delta \tag{11}$$

The fourth objective function J_4 estimates the discharging requirements of the EVs that opt-in to provide their energy to their assigned microgrids during the times when the grid faces higher demand, as follows:

$$J_4 = \sum \zeta_{ijn}\left(D^{EV-Disch}_{ijn}(t+k)\right).\Delta \tag{12}$$

The fifth objective functionJ_5 is the utility function associated with an EV*n*, connected to an aggregator *j* under microgrid *i*, as follows:

$$J_5 = \sum_{n\in N_{ijn}} U_{ijn}\left(D^{EV}_{ijn}\right) \tag{13}$$

Where

$$U_n\left(D^{EV}_{n}\right) = \mathscr{U}\left(\parallel D^{EV}_{n}\parallel_1\right) - \sum_{t\in\mathfrak{T}} V_n\left(D^{EV}_{n}(t)\right) \tag{14}$$

$$V_n(t+k) = C^{extra}_{ijn}(t+k).D^{EV}_{ijn}(t+k)] + \zeta_{ijn}(t+k)D^{EV,disch}_{ijn}(t+k) \tag{15}$$

$$\mathscr{U}\left(\parallel D^{EV}_{n}\parallel_1\right) = -\varphi\left(\parallel D^{EV}_{n}\parallel_1 - B_{ijn}\right)^2 \tag{16}$$

The battery degradation cost is found by the following expression [13,14]:

$$\zeta_{ijn}(t) = \alpha^1_{ijn}\left(D^{EV}_{ijn}(t)\right)^2 + \alpha^2_{ijn}\left(D^{EV}_{ijn}(t)\right) + \alpha^3_{ijn} \tag{17}$$

$$L\left(D^{EV}_{ijn},\lambda\right) = J + \sum_{J\in J_i}\sum_{n\in N^t_{ijn}} \lambda_{ijn}\cdot\left[B_{ijn} - \sum_{t\in\mathfrak{T}} D^{EV}_{ijn}\right] \tag{18}$$

$$B_{ijn} = \zeta_{ijn}\left[SoC^{dept\_mx}_{ijn} - SoC^{a}_{ijn}\right] \tag{19}$$

$$B_{ijn} = \xi_{ijn}\cdot\left[SoC^{dept\_mx}_{ijn} - SoC^{a}_{ijn}\right] \tag{20}$$

$$\lambda_{ijn} = C^{'*}_{ij}\left(D^{Base\_*}_{ijn}\right) + b^{'*}_{ij}\left(D^{EV\_*}_{ijn}\right) - \zeta^{'}_{ijn}\left(D^{EV,disch\_*}_{ijn}\right) \tag{21}$$

$$\lambda_{ijn} \geq C^{'*}_{ij}\left(D^{Base\_*}_{ijn}\right) + b^{'*}_{ij}\left(D^{EV\_*}_{ijn}\right) - \zeta^{'}_{ijn}\left(D^{EV,disch\_*}_{ijn}\right) \tag{22}$$

$$\begin{cases} eq(21),\ if\ D^{EV\_*}_{ijn} > 0 \\ eq(22),\ if\ D^{EV\_*}_{ijn} = 0 \end{cases} \tag{23}$$

For a group of EVs such that $n \in N^t_{ijn}$, the energy cost to meet the charging requirements for the *n*th EV under an aggregator *j* is formulated as follows:

$$J\left(D^{EV}_{ijn}, Pr(t)\right) = \sum_{t\in\mathfrak{T}} -\zeta_{ijn}(t).D^{EV,disch}_{ijn}(t) + Pr(t).D^{EV}_{ijn}(t) \tag{24}$$

Where $Pr(t)$ indicates the instantaneous charging price per each connected vehicle, and is broadcasted by microgrid *i* as follows:

$$Pr(t) = C^{*}_{ij}(t) + b^{*}_{ijn}(t) \tag{25}$$

Let us denote $D^{EV_*}_{ijn}$as the updated charging requirement for *n*th EV, then the *j*th aggregator that oversees the charging scheduling aims to minimize the per-vehicle charging cost as follows:

$$D^{EV\_*}_{ijn}(Pr(t)) = \underset{D^{EV}_{ijn}\in\mathscr{D}^{EV}}{argmin}\left[D^{EV}_{ijn}, Pr(t)\right] \tag{26}$$

Such that:

$$C^{*}_{ij}(t) = \sum_{J\in J_i} D^{B}_{ij}\ (t)\ .\ \left[C^{'}_{ij}\ (t)\right] + \omega_{ij}(t) \tag{27}$$

$$b^{*}_{ijn}(t) = \sum_{J\in J_i}\sum_{n\in N^t_{ijn}} D^{EV\_*}_{ijn}(t)\ .\ \left[b^{'}_{ijn}(t)\right] + \kappa_{ij}(t) \tag{28}$$

Both $\omega_{ij}(t)$ and $\kappa_{ij}(t)$ represent wheeling charges that resemble the cost of exchanging energy during time slot t with interconnected microgrids $\in I$, and with nearby stations. It should be noted that the first part of the summation in the equation represents the system. The charging requirements for a collection of EVs are updated in a decentralized manner. Such requirements depend mainly on arrival and requested departure SoC, parking duration, and the grid's operational status that dictates the energy prices based on the IDC curve that resembles the grid's instantaneous supply and demand levels. Specifically, the aggregator receives requests to charge the vehicles for the next timeslot. Each aggregator then sends the charging scheduling that includes the currently connected EVs and the newly introduced requests to its upstream microgrid. The associated microgrid then collects the updated scheduling of all aggregators beneath its authority and runs its centralized optimization problem based on both upstream and downstream inputs. Such inputs include other loads on its grid (non-EVs demand), power production from its generation unit and the upstream system operator, energy exchange among its nearby microgrids, transformer, and lines overloading conditions. After updating its IDC curve, each microgrid broadcasts a unique price signal for each of its attached aggregators. This price signal is composed of the power production price that is jointly determined with the upper layer (the system operator) and the marginal operation price that is determined for each aggregator by its assigned microgrid, as follows:

$$C^{(0)}_{ij}(t) = \left[C^{*}_{ij}(t);\ t\in\mathfrak{T}\right] \tag{29}$$

$$b^{(0)}_{ijn}(t) = \left[b^{*}_{ijn}(t);\ t\in\mathfrak{T}\right] \tag{30}$$

An iterative, offline, decentralized pricing mechanism, inspired by [15], is implemented in this work before the charging timeslot to identify the best pricing signal for each EV. Mainly, this mechanism considers the best charging requirement decision taken by each EV's owner, which is assumed to be influenced by the updated pricing signal. The decentralized mechanism works as following steps:

1 Initial power production and marginal operation prices, based on Eqs. (29) and (30).
2 Set

$$Pr^{(0)}(t) = \left[C^{(0)}_{ij}(t) + b^{(0)}_{ijn}(t);\ t\in\mathfrak{T}\right] \tag{31}$$

3 Set $h = 0$, $\epsilon = \epsilon_0$, such that $\epsilon_0 > 0$
4 For $\epsilon_0 > 0$, Execute the charging requirement decision $D^{EV\_(h+1)}_{ijn}$ with respect to $Pr^{(h)}(t)$, at an aggregator level as follows:

$$D^{EV\_(h+1)}_{ijn}\left(Pr^{(h)}(t)\right) = \underset{D^{EV}_{ijn}\in\mathscr{D}^{EV}}{argmin}\sum_{t\in\mathfrak{T}}\left[\zeta_{ijn}.\left(D^{EV,disch}_{ijn}(t) + b_{ijn}(t).D^{EV\_*}_{ijn}(t)\right]\right. \tag{32}$$

5 Each aggregator sends the charging requirement decisions of $D^{EV_(h+1)}_{ijn}$to its attached microgrid.

6 Each microgrid reports its total demand (EVs and non-EVs), and generation level as well as its committed power exchange with the system operator.

7 Based on the signal from the system operator, the microgrid updates its power production price (that includes any energy purchases from the upstream grid) as follows:

$$C_{ij}^{(h+1)}(t) = \sum_{J\in J_i} D_{ij}^{B_-*(h+1)}(t).\ \left[C_{ij}^{'}\right] + \omega_{ij}(t) \tag{33}$$

8 Each microgrid updates the pricing signal with respect to its instantaneous inverse-demand curve and operational status as follows:

$$b_{ijn}^{(h+1)}(t) = \sum_{j\in J_i}\sum_{n\in N_{ijn}^{t}} D_{ijn}^{EV_-*(h+1)}(t).\ \left[b_{ijn}^{'}\right] + \kappa_{ij}(t) \tag{34}$$

9 The microgrid broadcasts the charging prices per vehicle, based on the EV scheduling at aggregator j, as follows:

$$Pr^{(h+1)}(t) = C_{ij}^{(h+1)}(t) + b_{ijn}^{(h+1)}(t) \tag{35}$$

10 Update ϵ, as follows:

$$\epsilon = \sum_{j\in J_i} \parallel Pr^{(h+1)} - Pr^{(h)} \parallel \tag{36}$$

11 Update $h = h+1$, if needed,

3.2. Mathematical formulation of the upper-level based on the stackelberg model

Considering an oligopolistic energy market with a system operator that oversees a collection of microgrids, each microgrid has its generation units and has the capability of exchanging power (selling or receiving) with other interconnected microgrids. Let us assume that each microgrid has G generation units such that $g \in G$, with their marginal cost production at microgrid i is represented as C_i^gin \$/MWh with generation capacity x_i^gin *MWh*. The primal variables in the quadratic formulation, Ξ, are the output of generating units, the total demand, and the net energy exchange at microgrid i; $\Xi = \{x_i^g(t), D_i(t), \mathscr{L}_i(t)\}$.

One of the most efficient methodologies to solve a dual problem is the Wolfe dual. Let us consider a general maximization function $Max_x[g(x)|Z(x) \le 0]$, where $x \in R^n,\ g: R^n \to R,\ Z: R^n \to R^m$. The convex function, Z, and concave function g are assumed to be continuously differentiable. Let us introduce the Lagrangian function, $L(x,\lambda) = g(x) - \lambda^T Z(x)$, where the Lagrange multiplier $\lambda \in R^m$. The Wolfe dual could be expressed as $Min_{x,\lambda}\{L(x,\lambda)|\nabla_x L(x,\lambda) = 0, \lambda \ge 0\}$, with $\nabla_x L(x,\lambda)$ as the gradient values for x. It is worth mentioning that a strong duality exists between the Wolfe and primal values [16]. Given that an optimal solution has been reached, $\overline{x}$, and the primal satisfied the slater condition, then there exists $\overline{\lambda}$ s.t. $g(\overline{x}) = L(\overline{x},\overline{\lambda})$ that represent the optimal solution for the Wolfe dual problem. The dual Wolfe of the upper-level follower is formulated as follows:

$$\mathrm{F} = \sum_{\mathrm{f}=1}^{10} \mathrm{f} \tag{37}$$

Where

$$F_1 = \sum_{i\in I}\sum_{t\in\mathscr{T}}\left[C_i(t+h^{'}).D_i(t+h^{'}) - \frac{C_i(t+l)}{2\Gamma_i\ (t+l)}.\left[D_i(t+h^{'})^2 + \sum_{i\in I}\sum_{g\in G} x_i^g(t+h^{'})^2\right]\right].\Delta\ - \sum_{i,g\in G_{i,t}} C_i^g(t+h^{'}).x_i^g(t+h^{'}).\Delta \tag{38}$$

The objective function, F_1, intends to maximize the social welfare of the consumers. At a timeslot t, the first part of the objective function sums the integral of the area covered under the IDC curve, which is subtracted by the second part which represents the energy generation costs at microgrid i level. Γ_i represents the cumulative capacity in MW in the inverse-demand curve, D_i represents the total demand at microgrid i that include, at this level of the optimization problem, both the EVs and non-EVs loads.

$$F_2 = \sum_{i,g\in G_{i,t}} \Upsilon_i^g(t+h').[x_i^g(t+h') - \mathfrak{X}_i^g].\Delta \tag{39}$$

The objective function (39) represents the net summations of capacity scarcity exchange on microgrid i during a timeslot t. Here, Υ_i^g represents the scarcity cost of unit g in microgrid i, which is the marginal opportunity cost imposed on future generations on the unit.

$$F_3 = \sum_{s,t}\lambda_s^{+}(t+h').\left[\sum_i \mathbb{Y}_{s,i}.\mathscr{L}_i(t+h') - \mathbb{Z}_s\right].\Delta \tag{40}$$

$$F_4 = \sum_{s,t}\lambda_s^{-}(t+h').\left[-\sum_i \mathbb{Y}_{s,i}.\mathscr{L}_i(t+h') - \mathbb{Z}_s\right].\Delta \tag{41}$$

Here, $\mathbb{Y}_{s,i}$ is a matrix representation of the reciprocal of the grid's reactance between microgrids *i and j*. It is worth mentioning that in case of a power transfer between the microgrids, the column that represents the supplier microgrid is filled with zero entries to represent the node as a sink bus. Furthermore, matrix $\mathbb{Y}_{s,i}$is multiplied by either a positive or negative sign in a way that defines the direction of the power flow, with subscript s representing the flow between microgrids (*i,j*), while the subscript *i* indicates such flow is seen as either positive or negative from the ith microgrid. On the other hand, $\mathscr{L}_i$ is a variable that represents the net energy mass balance of receiving and delivering power at the microgrid during a timeslot t. Its multiplication of matrix $\mathbb{Y}_{s,i}$ indicates the upper and lower limits on the transmission line between microgrids i and j. Finally, $\mathbb{Z}_s$ represents the MW capacity limit of the transmission line between any two microgrids in the system.

$$F_5 = \sum_{i\in I}\sum_{t\in\mathscr{T}} C_i(t+l).\left[\mathscr{L}_i(t+h') - \sum_{l,g\in G_{l,t}} x_{li}^g(t+h') + D_i(t+h')\right].\Delta \tag{42}$$

$$F_6 = \sum_{t\in\mathscr{T}}\varphi_i(t+h').\left[-\sum_{i\in I}\mathscr{L}_i(t+h')\right].\Delta \tag{43}$$

The objective functions (42) and (43) quantify the total marginal price of each microgrid as a result of energy transmission charges between different microgrids. Specifically, the microgrid's locational marginal price C_i, is composed of both the system price φ_i because of generating or purchasing/selling power, and wheeling charge, $\omega_i(t)$ that represents the charges accumulated for utilizing the network to transfer power when the grid is congested. Such charges could be represented as follows:

$$\omega_i(t) = C_i(t) - \ \varphi_i(t) \tag{44}$$

The objective function (45) is formulated to regulate the carbon emission in the system, as follows:

$$F_7 = p^{co}\left[\sum_{l,i,g\in G_{l,i,t}} G_{li}^{co}.x_{li}^g.\Delta - \ \overline{G}\right] \tag{45}$$

Where p^{co} represents the CO_2 permit price that each microgrid must pay with respect to the level of emissions from its generating units. G_{li}^{co} represents the rate of CO_2 emission from microgrid i during timeslot t, subscript l refers to the system operator as a leader, $\overline{G}$ is the emission's cap level, established by the system's operator with respect to the operational status of the system. Transfer of MW between microgrids i *and* m affect directly the linear inverse-demand curve at both microgrids. Therefore, the elasticity price as a result of changes in both microgrids' x-axis levels is described as follows:

$$F_8 = \sum_{m,i,g\in G_{m,i,t}} \mathscr{E}_{mig}(t+l).(-x_{mi}^{g}(t+h')).\Delta \tag{46}$$

Where

$$\varepsilon_{mi} = \frac{\frac{\pm\Gamma_i^{'}}{\Gamma}}{\frac{\pm C_i^{'}}{C}} \tag{47}$$

$$F_9 = p_{REP}\left[\sum_{i\in I}\sum_{q\in Q_i} x_i^{q}(t).\Delta - \Omega\left[\sum_{i\in I}\sum_{g\in G_i} x_i^{g}(t).\Delta\right]\right] \tag{48}$$

The objective function (48) represents the RPS requirement per microgrid at the interconnected system. Furthermore, an RPS level of the total generation sources is assumed to be mandated by the local authority so that a specific percentage, Ω, of the total generation must be incorporated from generators q that belong to a set of renewable energy sources Q_i. p_{REP} represents the monetary obligations per microgrid, with its signs as an indication of whether the microgrid is selling (positive) or receiving (negative) energy from renewable energy sources from a nearby microgrid. The emission cost is neglected in the case of RPS certification trading since renewable sources do not emit any CO_2 in the generation process. Finally, the availability of energy to provide to nearby stations is represented as the capacity level each microgrid has after the implementation of the optimization problem in the previous timeslot, as follows:

$$F_{10} = \sum_{i\in I}\sum_{t\in\mathscr{J}} \mathscr{A}_i(t+h').\Delta \tag{49}$$

The objective function (37) is minimized with respect to the variables in $\Xi = \{x_i^g(t), D_i(t), \mathscr{L}_i(t)\}$, and $\Psi = \{\mathrm{Y}_i^g(t), \boldsymbol{\lambda}_s^+(t), \boldsymbol{\lambda}_s^-(t), w_i(t), \psi_i(t), \rho, \boldsymbol{\varepsilon}_i^g(t), \Omega_i(t)\}$. The gradients of the lagrangian drive the following conditions with respect to Ξ:

$$\left[-\frac{C_i^{'}(t)}{\Gamma_i^{'}(t)}\sum x_i(t) - C_i^{g}(t) - \mathrm{Y}_i^{g}(t) + w_i(t) - \rho G_i^{co2,g}(t) + \varepsilon_i^{g}(t)\right]\Delta_t = 0 \tag{50}$$

$$\left[C_i(t) - \frac{C_i^{'}(t)}{\Gamma_i^{'}(t)}D_i(t) - w_i(t) + \Omega_i(t)\right]\Delta_t = 0 \tag{51}$$

$$\left[-\sum_s\left(\lambda_s^+(t) - \lambda_s^-(t)\right)\mathbb{Y}_{s,i} - w_i(t) + \psi_i(t)\right]\Delta_t = 0 \tag{52}$$

$$\mathrm{Y}_i^{g}(t) \geq 0 \tag{53}$$

$$\boldsymbol{\lambda}_s^+(t) \geq 0 \tag{54}$$

$$\boldsymbol{\lambda}_s^-(t) \geq 0 \tag{55}$$

$$\rho \geq 0 \tag{56}$$

$$\boldsymbol{\varepsilon}_i^{g}(t) \geq 0 \tag{57}$$

$$\Omega_i(t) \geq 0 \tag{58}$$

$$\forall\ s \in S,\ g \in G_i, i \in I,\ t \in T$$

It is worth mentioning that nonnegativity constraints are placed on the variables that are associated with the inequality constraints, $\{\mathrm{Y}_i^g(t), \lambda_s^+(t), \lambda_s^-(t), \rho, \varepsilon_i^g(t), \Omega_i(t)\}$; otherwise, variables in the quadratic representation are non-restricted. Δ_t is multiplied by the left-hand side to account for the hourly value of each dual variable.

The upper level that represents the system's operator at the first layer could be modeled similarly as follows:

$$\sum_{i\in I}\sum_{g\in G_l}\left[C_i(t+h') - C_{li}^{g}(t+h') - p^{co}G_{li}^{co} - \right]\ x_{li}^{g}(t+h').\Delta \tag{59}$$

$$\mathscr{R} = \mathscr{R}_1 - [\mathscr{R}_2 + \mathscr{R}_3 + \mathscr{R}_4 + \mathscr{R}_5 + \mathscr{R}_6] \tag{60}$$

$$\mathscr{R}_1 = \sum_{i,t}\left[C_i^{'}(t+h').D_i(t+h') - \frac{C_i^{'}(t+h')}{\Gamma_i(t+h')}\left(D_i(t+l)^2\right)\right].\Delta \tag{61}$$

$$\mathscr{R}_2 = \sum_{m,i,g\in G_{mi,t}}\left[\frac{C_i^{'}(t+h')}{\Gamma_i(t+h')}.\sum_{(g',g)\in G_{mi}} x_{mi}^{g'}(t+h').x_{mi}^{g}(t+l)\right].\Delta \tag{62}$$

$$\mathscr{R}_3 = \sum_{m,i,g\in G_{mi,t}} C_{li}^{g}(t+h').x_{li}^{g}(t+h').\Delta \tag{63}$$

$$\mathscr{R}_4 = \sum_{s,t}\left[\lambda_s^+(t+h') + \lambda_s^-(t+h')\right].\mathbb{Z}_s.\Delta - p^{co}\overline{G} \tag{64}$$

$$\mathscr{R}_5 = \sum_{m,i,g\in G_{mi,t}} \mathrm{Y}_{mi}^{g}(t+h').\mathfrak{X}_{mi}^{g}.\Delta \tag{65}$$

$$\mathscr{R}_6 = p_{REP}\left[\sum_{q\in Q_l} x_{li}^{q}(t).\Delta - \Omega\left[\sum_{g\in G_l} x_{li}^{g}(t).\Delta\right]\right] \tag{66}$$

We linearize the complimentary conditions found in the previous equations via disjunctive constraints [17], as follows:

$$0 \leq -[x_i^g(t) - X_i^g(t)]\Delta_t \leq M^1 r_i^{g,1}(t) \tag{67}$$

$$0 \leq \mathrm{Y}_i^g(t) \leq M^1\left(1 - r_i^{g,1}(t)\right) \tag{68}$$

$$0 \leq -\left[-\sum_i \mathbb{Y}_{s,i}\mathscr{L}_i(t) - \mathbb{Z}_s\right]\Delta_t \leq M^2 r_s^2(t) \tag{69}$$

$$0 \leq \lambda_s^+(t) \leq M^2\left(1 - r_s^2(t)\right) \tag{70}$$

$$0 \leq \lambda_s^-(t) \leq M^3\left(1 - r_s^3(t)\right) \tag{71}$$

$$0 \leq -\left[-\mathbb{Y}_{s,i}\mathscr{L}_i(t) - \mathbb{Z}_s\right]\Delta_t \leq M^3 r_s^3(t) \tag{72}$$

$$0 \leq -\left[\sum_{g,i\in Gi,t} G_i^{co2,g}x_i^g(t)\Delta_t - \overline{G}\right] \leq M^4 r^4 \tag{73}$$

$$0 \leq \rho \leq M^4\left(1 - r^4\right) \tag{74}$$

$$0 \leq x_i^g(t)\Delta_t \leq M^5\left(1 - r_i^{g,5}(t)\right) \tag{75}$$

$$0 \leq D_i(t)\Delta_t \leq M^6 r_i^{g,6}(t) \tag{76}$$

$$0 \leq \Omega_i(t) \leq M^6\left(1 - r_i^{g,6}(t)\right) \tag{77}$$

$$0 \leq -\left[-\mathbb{Y}_{s,i}\mathscr{L}_i(t) - \mathbb{Z}_s\right]\Delta_t \leq M^3 r_s^3(t) \tag{78}$$

$$0 \leq -\left[\sum_{g,i\in Gi,t} G_i^{co2,g}x_i^g(t)\Delta_t - \overline{G}\right] \leq M^4 r^4 \tag{79}$$

$$r_i^{g,1}(t) \in \{0,1\} \tag{80}$$

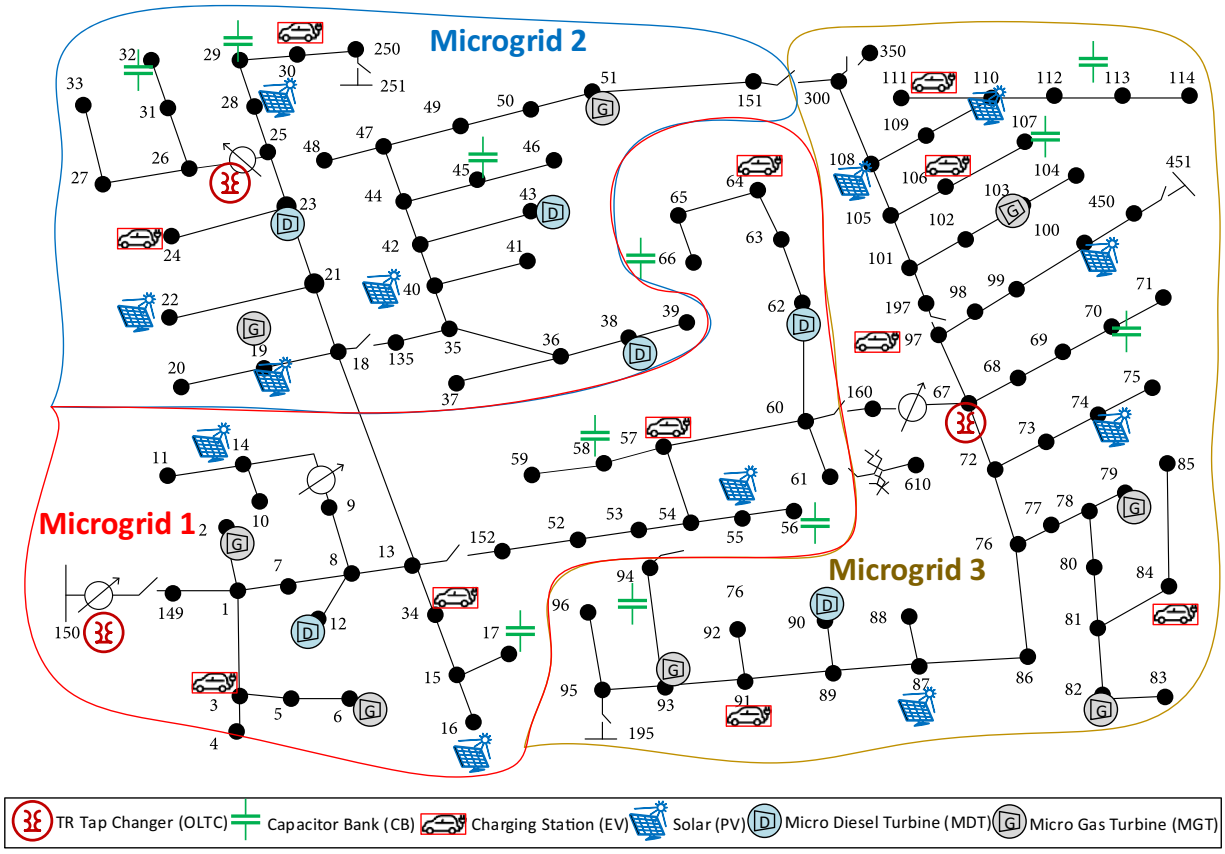

Fig. 3. The modified IEEE 123 test system with the energy grid information.

$$r_s^2(t) \in \{0,1\} \tag{81}$$

$$r_s^3(t) \in \{0,1\} \tag{82}$$

$$r^4 \in \{0,1\} \tag{83}$$

$$r_i^{g,5}(t) \in \{0,1\} \tag{84}$$

$$r_i^{g,6}(t) \in \{0,1\} \tag{85}$$

$\forall\ s \in S,\ g \in G_i, i \in I,\ t \in T$

The set $\Pi = \{r_i^{g,1}(t), r_s^2(t), r_s^3(t), r^4, r_i^{g,5}(t), r_i^{g,6}(t)\}$ represents the binary variables in this work, associated with the big-M method constants $\{M^1, M^2, M^3, M^4, M^5, M^6\}$. The system operator projects revenue from selling energy to the downstream level of microgrids minus the operational costs. Such operational costs include the costs of the CO_2 and RPS permits imposed by state or local regulators. To obtain an optimal solution to the microgrid's layer, variables of the system operator's layer need to be fixed. This allows the representation of the optimal primal and dual solutions at the microgrid level as functions of $x_i^g(t+1)$. The objective function given in Eq. (60) is now a convex MIQP function, with linear equalities and inequalities constraints. It could be solved using a commercial optimization toolbox such as CPLEX and Gurobi.

4. Case study

In order to test the effectiveness of the proposed tri-level hierarchical control of energy management considering large-scale integration of EVs, case studies were carried out on the modified IEEE 123 bus system. The case studies considered the optimal decomposition of this test system into three partitions, as discussed in [18]. This work assumes that a microgrid operates each partition. Thus, the system operator is dealing with three microgrids, each has four charging stations within its jurisdiction.

Table 1
System generation-related parameters.

Unit	No of Gen Units	Capacity	Marginal Cost	Capacity Factor	CO_2 emission rate
MGT	5	250 kW	0.199	0.72	02 kg.Cos /KWh
MDT	5	250 kW	0 125	0.72	0.28
PV	10	75 kW (4) 100 kW (4) 125 kW (3)	0	0.28	0

4.1. Description of the test system

Fig. 3 presents an illustration of the modified IEEE 123 bus system with the incorporation of three microgrids. The system information is given in Table 1. The resistive and inductive parameters of the lines are set to be 0.05 and 0.11 per unit, while the system's base MVA is 100 [19]. The system includes ten PV units with different capacities, five 250 kW gas-fired microturbines, and five 250 kW diesel-fired microturbines. The generation units' marginal and emission costs are adopted from [20] and are labeled in Table 1. The total load on the system is 3.8 MW. As stated earlier, when a microgrid reaches its maximum generation capability, it can purchase power from either the upstream grid, which is run by the system operator, or from its neighboring microgrids, based on information supplied by the system operator. The wheeling charge is assumed to be set as 4 $/MWh for low voltage access to the

Table 2
Comparisons between the proposed framework vs. benchmarks.

Generation Output (MWh)	PC [24]	Cournot [25]	Proposed work
System operator	84.21	87.25	85.45
MG1	19.52	17.43	17.92
MG2	16.35	15.4	16.12
MG3	20.83	20.95	21.95
Total	140.91	141.03	141.44
CO_2 emissions [kt]	2500	2500	2500
Permit price [$/kt]	1500	890	1000

transmission system, and is adopted from the California Independent System Operator (CAISO) [21].

4.2. Simulation results

The results of the proposed tri-level structure show that the proposed system can efficiently coordinate the energy management of the electric grid, taking into consideration the large-scale integration of EVs. The arrival and departure of the EVs into the charging station are beyond the scope of this work; therefore, we adopt them based on the well-established studies in [22,23].

As mentioned earlier, the system operator acts as a leader in the Stackelberg hierarchy, while the microgrid operators act as followers. The emission cap is set in this work at 2500 kt. The solutions were obtained based on solving the MIQP function. To show the proposed hierarchy's effectiveness, we compare the obtained results versus the normalized results of the previously published energy management framework. Table 2 shows the effectiveness of the proposed framework in this work. As noted, the production output is less than the perfect competition (PC) [24] and Cournot-based [25] frameworks, since the latter surpasses the generation levels to increase their revenue margins. Nevertheless, the results show that the operational revenue under our proposed methodology is the highest, indicating an optimal combination of the generation resources and power exchange to reduce CO_2 emissions costs. Furthermore, it is noted that the proposed hierarchy successfully minimizes the price of CO_2 permits since the operator allows the exchange of energy to reduce dependence on diesel-fired generation units that emit a higher level of CO_2.

As results shown in Fig. 4 indicate, MG1 and MG2, which integrate four diesel units on their premises, buy energy from MG3, request energy discharge from EV consumers, and request energy support from the upstream network to support a certain amount of power rather than generating them from their diesel-fired generation units. As a result of the decentralized charging algorithm, the energy prices successfully influence the EVs owners to postpone their charging. It is worth mentioning that the proposed hierarchy, driven by the need to meet a certain RPS percentage per microgrid, allows more energy exchange. Indeed, and due to the carbon cap-and-trade implementation, it would be more cost-efficient for MG1 to buy energy from MG3 than to produce it from its diesel-fired microturbines.

As shown in Table 3, the proposed hierarchy successfully led to reduced energy pricing throughout the day. It is worth mentioning that prices vary per microgrid as a result of the variety of generation levels of its distributed generators. It is noted from the presented results in Table 3 that as a result of the energy exchange that both MG1 and MG2 perform during peak demand hours, their peak energy prices are slightly higher than those at MG3. This is contributed mainly to the wheeling charges illustrated in (44) in this work. The wheeling charges have no effect in the off-peak period since the level of congestion on the lines is significantly lower than during peak demand hours. Additionally, it is worth mentioning that if the modified test system has higher congestion capacity, then the wheeling charges would have been significantly diminished during peak demand hours, and accordingly the energy prices during these time frames. Also, it is widely evident that the Cournot model would yield higher energy prices since this type of energy market would lead to lower energy generation output and exchanges to drive the energy prices upward and obtain higher profits accordingly. This contributes to the proposed model surpassing the Cournot model in terms of social welfare to average consumers.

Table 3
Peak and off-peak energy prices for the benchmark simulations.

	PC		Co		Ours	
Energy price ($/KWh)	Peak	Off-peak	Peak	Off-peak	Peak	Off-peak
System operator	0.214	0.152	0.191	0.142	0.165	0.091
MGI	0.192	0.154	0.11	0.155	0.16	0 105
MG2	0.201	0.145	0.178	0.147	0.171	0.11
MG3	0.188	0.134	0 169	0.125	0 147	0.082

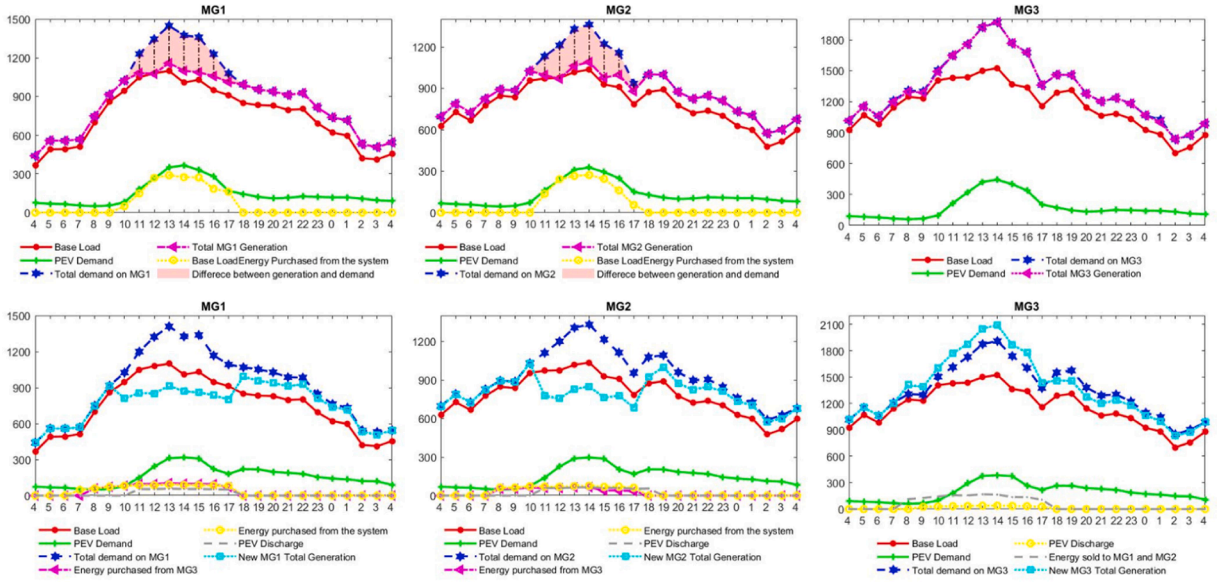

Fig. 4. System's operation before (upper) and after (lower) the implementation of the proposed framework.

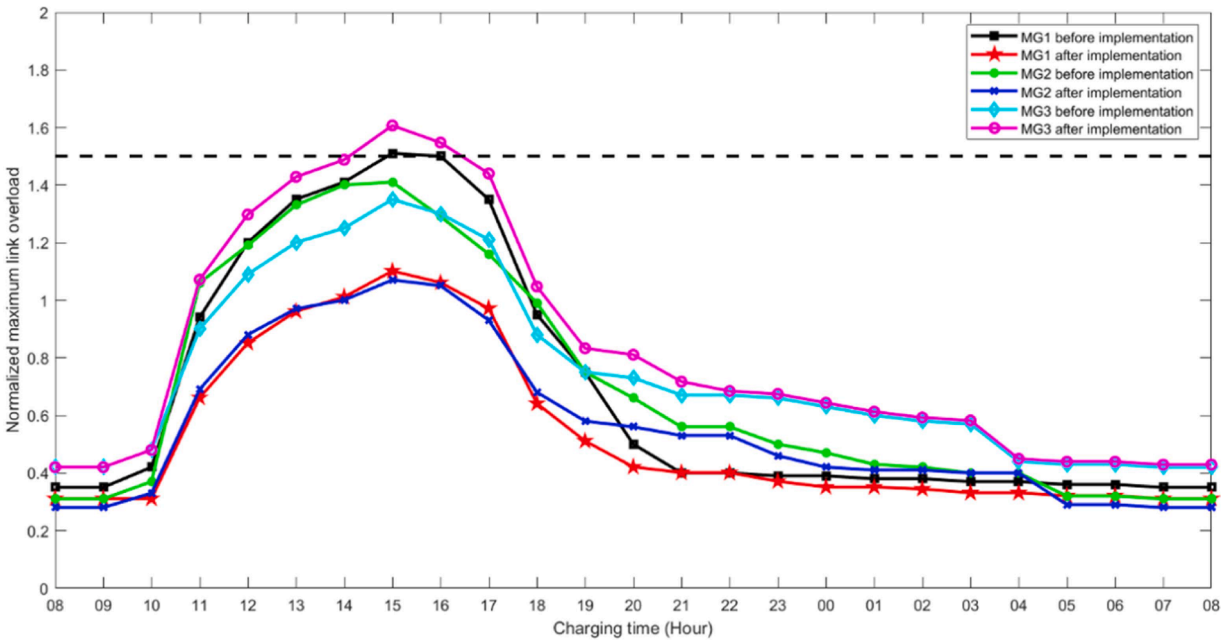

Fig. 5. System overloading conditions before and after the implementation of the proposed strategy.

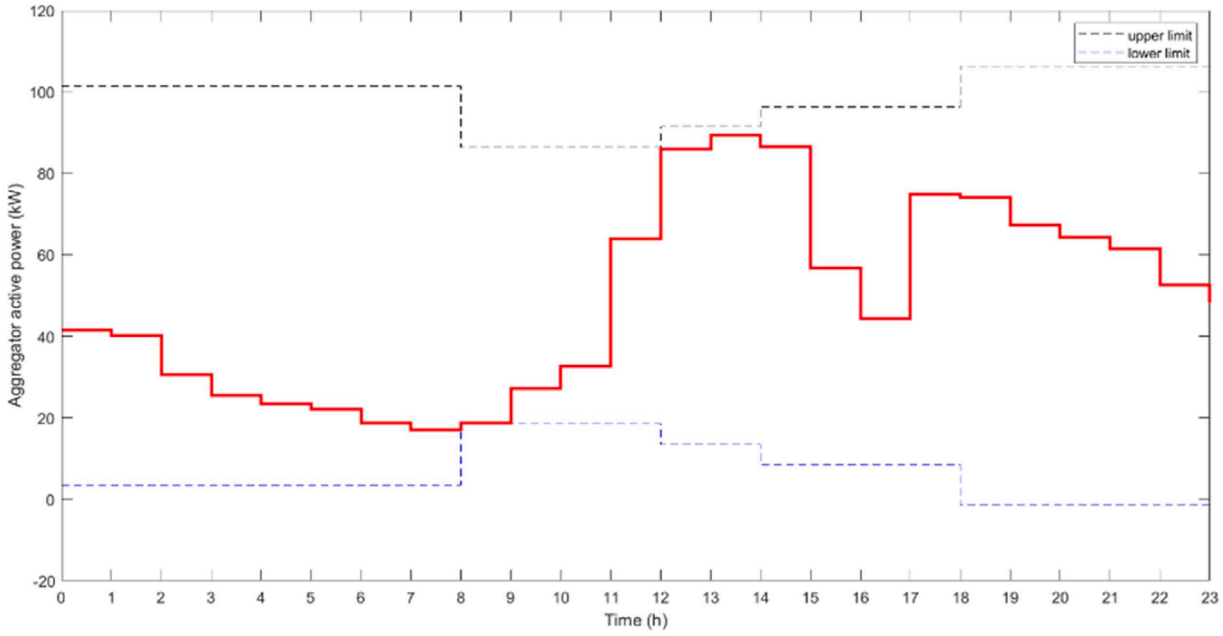

Fig. 6. Upper and lower limits of aggregator A of microgrid no.1.

Furthermore, it shows the effectiveness of shifting the EVs loads into off-peak demands following the implementation of the proposed strategy. Results in Fig. 5 show the impact of the updated aggregated charging needs of the EVs owners as a result of implementing the proposed framework. It illustrates the charging loads after the implementation of the control strategy that dispatches accurate energy price signals based on the network condition considering the inelasticity of the base demand. Specifically, implementation shows that both power transformers at MG1 and MG2 violate their capacity limitations. Additionally, Fig. 6 shows the impact of the proposed strategy on both energy and power requests on a station's aggregator under MG2. Specifically, each aggregator has an upper and lower limit dictated by its attached microgrid. During the peak hours, and by implementing the discharging price offer illustrated in Eq. (12), the aggregator's limit moves up in values, as positive values in the figure indicate energy supply to MG2 during the peak demand hours windows. Accordingly, incorporating the TRs capacity into the pricing scheme has forced a good amount of EVs to postpone their vehicles charging which successfully led to the flattening of the charging curve.

5. Conclusion

This work proposes a tri-level, hierarchical energy management coordination mechanism that optimally manages the electric network considering large-scale integration of the EVs. This framework's central concept is based on establishing energy price signals by following the timely updates of the inverse-demand curve. This work realizes that utilizing the inverse-demand function is the best strategy to produce

accurate and supply-influenced energy prices. Such a claim is valid since its price estimation accounts for any slight modification in the supply quantity (system's energy generation) and demand of products (consumers' utilization of energy). That is to say; the tri-level energy optimization problem took into account various operational and policy constraints that are imposed on the real-life operation of the system. Such restrictions include line and transformer overloading, RPS requirement, carbon emission requirement, and EVs charging and discharging limitations due to the system's condition. The formulation of the proposed framework was achieved by MIQP representation, and KKT and big M-method approximations were performed to ensure accurate implementation of the electrical energy system's constraints, where there is a need to account for its non-linearity nature. The IEEE 123 bus system was used to test the proposed tri-level framework. Furthermore, this work assumed three microgrid entities directly connected to a system operator at its upper-level layer and charging stations run by aggregators at its lower-level layer. The reason behind such dissection lies in the results obtained in [18], where optimal decomposition of the system into partitions based on their voltage, active and reactive power limits was performed. Finally, results show that successful implementation of the proposed framework led to influencing the charging behavior of hundreds of the EVs owners to delay their charging requirements due to the dynamic energy price signals that are issued based on the system's timely operation. Additionally, the results show the optimal energy exchange between different microgrids to support their overall operation and reduce the overall cost incurred from their generation units.

CRediT authorship contribution statement

Tawfiq Aljohani: Conceptualization, Data curation, Formal analysis, Investigation, Methodology, Software, Validation, Visualization, Writing – original draft, Writing – review & editing. **Mohamed A. Mohamed:** Methodology, Validation, Visualization, Supervision, Writing – review & editing. **Osama Mohammed:** Conceptualization, Data curation, Formal analysis, Investigation, Methodology, Supervision, Writing – review & editing.

Declaration of Competing Interest

The authors declare no conflict of interest.

Data availability

No data was used for the research described in the article.

Acknowledgement

The authors extend their appreciation to the Deputyship for Research & Innovation, Ministry of Education in Saudi Arabia for funding this research work through the project number 445-9-221.

References

[1] Hadley, S.W. (2006). Impact of plug-in hybrid vehicles on the electric grid. ORNL Report, (October).
[2] M.M. Collins, G.H. Mader, The timing of EV recharging and its effect on utilities, IEEE Trans. Veh. Technol. 32 (1) (1983) 90–97.
[3] T. Aljohani, O. Mohammed, Modeling the impact of the vehicle-to-grid services on the hourly operation of the power distribution grid, Designs 2 (2018) 55.
[4] A.H. Hajimiragha, C.A. Canizares, M.W. Fowler, S. Moazeni, A. Elkamel, A robust optimization approach for planning the transition to plug-in hybrid electric vehicles, IEEE Trans. Power Syst. 26 (4) (2011) 2264–2274.
[5] J. Hu, S. You, M. Lind, J. Østergaard, Coordinated charging of electric vehicles for congestion prevention in the distribution grid, IEEE Trans. Smart Grid 5 (2) (2013) 703–711.
[6] S.J. Gunter, K.K. Afridi, D.J. Perreault, Optimal design of grid-connected PEV charging systems with integrated distributed resources, IEEE Trans. Smart Grid 4 (2) (2013) 956–967.
[7] F. Ni, L. Yan, K. Wu, M. Shi, J. Zhou, X. Chen, Hierarchical optimization of electric vehicle system charging plan based on the scheduling priority, J. Circuits Syst. Comput. 28 (13) (2019), 1950221.
[8] K. Kaur, M. Singh, N. Kumar, Multiobjective optimization for frequency support using electric vehicles: an aggregator-based hierarchical control mechanism, IEEE Syst. J. 13 (1) (2017) 771–782.
[9] V.H. Bui, A. Hussain, H.M. Kim, A multiagent-based hierarchical energy management strategy for multi-microgrids considering adjustable power and demand response, IEEE Trans. Smart Grid 9 (2) (2016) 1323–1333.
[10] B. Shakerighadi, A. Anvari-Moghaddam, E. Ebrahimzadeh, F. Blaabjerg, C.L. Bak, A hierarchical game theoretical approach for energy management of electric vehicles and charging stations in smart grids, IEEE Access 6 (2018) 67223–67234.
[11] Y. Zou, Y. Dong, S. Li, Y. Niu, Multi-time hierarchical stochastic predictive control for energy management of an island microgrid with plug-in electric vehicles, IET Gener. Transm. Distrib. 13 (10) (2019) 1794–1801.
[12] I.S. Bayram, M. Abdallah, K. Qaraqe, Providing QoS guarantees to multiple classes of EVs under deterministic grid power, in: Proceedings of the 2014 IEEE International Energy Conference (ENERGYCON), IEEE, 2014, pp. 1403–1408.
[13] A. Ahmadian, M. Sedghi, B. Mohammadi-ivatloo, A. Elkamel, M.A. Golkar, M. Fowler, Cost-benefit analysis of V2G implementation in distribution networks considering PEVs battery degradation, IEEE Trans. Sustain. Energy 9 (2) (2017) 961–970.
[14] Z. Ma, S. Zou, X. Liu, A distributed charging coordination for large-scale plug-in electric vehicles considering battery degradation cost, IEEE Trans. Control Syst. Technol. 23 (5) (2015) 2044–2052.
[15] Z. Ma, D.S. Callaway, I.A. Hiskens, Decentralized charging control of large populations of plug-in electric vehicles, IEEE Trans. Control Syst. Technol. 21 (1) (2011) 67–78.
[16] L.M. Dudkin, I. Rabinovich, I. Vakhutinsky, M.R. Dekker, Fletcher: Practical Methods of Optimization, Wiley, Chichester, 1987, p. 436, xiv+pagesc2450ISBN O-471-91547-5.
[17] J. Fortuny-Amat, B. McCarl, A representation and economic interpretation of a two-level programming problem, J. Oper. Res. Soc. 32 (9) (1981) 783–792.
[18] T.M. Aljohani, A.A.S. Ahmed, O.A. Mohammed, Two-stage optimization strategy for solving the VVO problem considering high penetration of plug-in electric vehicles to unbalanced distribution networks, IEEE Trans. Ind. Appl. (2021).
[19] IEEE 123 Node Test Case. (2019, October 16). Retrieved July 07, 2020, from https://xendee.com/ieee-123-node-test-case/.
[20] Quaschning, V. (n.d.). Specific carbon dioxide emissions of various fuels. Retrieved January 03, 2021, from https://www.volker-quaschning.de/datserv/CO2-spez/index_e.php.
[21] Quick and accurate settlements help market function. 2023 California ISO - Settlements. Retrieved from http://www.caiso.com/market/Pages/Settlements/Default.aspx.
[22] K. Knezović, A. Soroudi, A. Keane, M. Marinelli, Robust multi-objective PQ scheduling for electric vehicles in flexible unbalanced distribution grids, IET Gener. Transm. Distrib. 11 (16) (2017) 4031–4040.
[23] K. Knezović, M. Marinelli, Phase-wise enhanced voltage support from electric vehicles in a Danish low-voltage distribution grid, Electric Power Syst. Res. 140 (2016) 274–283.
[24] T. Matsumura, A. Yamagishi, Long-run welfare effect of energy conservation regulation, Econ. Lett. 154 (2017) 64–68.
[25] A. Penkovskii, V. Stennikov, E. Mednikova, I. Postnikov, Search for a market equilibrium of Cournot-Nash in the competitive heat market, Energy 161 (2018) 193–201.